Practical Computation of the Charge Mobility in Molecular Semiconductors Using Transient Localization Theory

Tahereh Nematiaram,*[1] Sergio Ciuchi,[2] Xiaoyu Xie,[1] Simone Fratini,[3] Alessandro Troisi[1]

[1]Department of Chemistry and Materials Innovation Factory, University of Liverpool, Liverpool L69 7ZD, U.K.

[2]Department of Physical and Chemical Sciences, University of L'Aquila, Via Vetoio, I-67100 L'Aquila, Italy

[3]Institut Néel, CNRS and Université Grenoble Alpes, Grenoble F-38042, France

*E-mail: *Tahereh.Nematiaram@liverpool.ac.uk*

Abstract

We describe a practical and flexible procedure to compute the charge carrier mobility in the transient localization regime. The method is straightforward to implement and computationally very inexpensive. We highlight the practical steps and provide sample computer codes. To demonstrate the flexibility of the method and generalize the theory, the correlation between the fluctuations of the transfer integrals is assessed. The method can be transparently linked with the results of electronic structure calculations and can therefore be used to extract the charge mobility at no additional cost.

1. Introduction

The mechanism of charge transport in molecular semiconductors is highly debated and already the topic of several recent reviews[1–6]. The community is gradually converging toward the idea that the charge carrier dynamics in the molecular semiconductor is strongly coupled with low-frequency nuclear motions that modulate the intermolecular coupling and is ultimately determined by them[7–9]. Because of the similarity between the energy scales of intermolecular transfer integral, phonon energy and thermal energy the quantum dynamics for these systems is extremely challenging to model and a family of alternative method is emerging[10–20]. Building on existing numerical evidence, an alternative approach that avoids explicit quantum dynamics simulation (cf. Refs.[21–26]) was originally introduced by Fratini et al, and benchmarked on a one-dimensional model, where it was shown to reproduce the main qualitative features of transport[6]. It is based on the observation that the large amplitude thermal molecular motions act as a source of dynamical disorder leading to a "transient localization" of the wavefunctions on timescales shorter than the period of molecular oscillations $\tau(=\hbar/\omega_0)$ which strongly restrict the carrier diffusion. As will be explained later, the main assumption in the transient localization theory is the relaxation time approximation, i.e., the idea that the dynamical properties of the electronic system, described by current-current anticommutator correlation function $C_+(t)$, can be expressed in terms of those of a reference system ($C_+^{ref}(t)$) from which it decays over the time ($C_+(t)=C_+^{ref}(t)e^{-t/\tau}$). The reference system is the organic semiconductor with only static disorder, i.e., with frozen molecular displacements. At a time shorter than τ (e.g., ($t=\hbar/J$) set by the inter-molecular transfer integrals) the system will not be distinguishable from the static disorder case because the molecular motions appear as frozen at such short time scales. As a result, the electronic and transport properties of the organic semiconductor can be directly inferred from the study of a reference system with frozen molecular displacements, i.e., a time-independent Hamiltonian. When this theory was applied to a range of realistic materials using parameters computed from electronic structure calculations it proved able to predict quite accurately the charge mobility of single crystalline molecular semiconductors[27].

Solving for the reference system still requires the exact evaluation of the electron dynamics in a disordered environment, which must be done numerically. In Ref. 27, this was achieved via the direct computation of the time-dependent quantum spread $\Delta X^2(E,t) = \left\langle [\hat{X}(t) - \hat{X}(0)]^2 \right\rangle_E$ of electrons, using a real-space method based on orthogonal polynomials[28]. This method was originally devised to deal very efficiently with large system sizes, of up to 10^6 orbitals. However, given the rather short localization lengths characteristic of organic semiconductors, typically in the range of few to few tens of molecules, the required accuracy is expected to be within reach of more standard methods of much simpler implementation.

The majority of computational works addressing the charge transport properties of molecular semiconductors with a variety of methods produces the parameters required for the evaluation of the mobility using transient localization theory. In this work, we present the simplest possible methodology to perform such calculation at a virtually negligible additional cost (sample computer codes are also provided). The associated code is distributed freely and we believe it has a great potential to screen high-mobility materials and possibly to increase the pace of material discovery. The theory can be linked with first principle calculations of the solid-state model Hamiltonian[29–33] or semi-classical molecular dynamics/quantum chemistry evaluation of the model[34–38], i.e., the two main families of computational methods used so far. In the presentation, we highlight the practical steps of the procedure and some numerical considerations. We also generalize the theory to allow for correlation in the fluctuation of the transfer integral between different pairs of molecules and discuss the impact of such generalization on the computed mobility. The transfer integrals correlation is very frequently invoked in case of static disorder in organics[39] and explicitly discussed in some work on molecular crystals[40]. In this paper, we provide a quantitative mean to quantify their importance both in model and realistic systems.

The paper is organized as follows. We first define the parameters of the model with a discussion on how they can be obtained from computational method. We then provide an outline of the transient localization method followed by a number of examples.

2. Methodology

Background Theory and Definitions

We consider a standard tight-binding Hamiltonian for molecular semiconductors,

$$\hat{H} = \sum_i \varepsilon_i \hat{c}_i^+ \hat{c}_i + \sum_{<ij>} J_{ij}^0 \hat{c}_i^+ \hat{c}_j + \sum_l \hbar\omega_l (\hat{a}_l^+ \hat{a}_l + \frac{1}{2}) + \sum_{i,l} g_i^l \frac{1}{\sqrt{2}} (\hat{a}_l^+ + \hat{a}_l) \hat{c}_i^+ \hat{c}_i + \sum_{i \neq j,l} g_{ij}^l \frac{1}{\sqrt{2}} (\hat{a}_l^+ + \hat{a}_l) \hat{c}_i^+ \hat{c}_j \quad (1)$$

where the first two terms indicate the electronic part of the Hamiltonian, the third term describes the lattice phonons, and the last two terms correspond to local and non-local electron-phonon couplings; ε_i represents the on-site electronic energy of the hole (the trivial changes required to described electrons as mentioned below); J_{ij}^0 the transfer integral elements between adjacent molecules at the equilibrium geometry; $\hat{c}_i^+(\hat{c}_i)$ the creation (annihilation) operator for a hole at site i (there is one state per site); $<ij>$ nearest-neighbour pairs of occupied sites; $\hbar$ the reduced Planck constant; ω_l the phonon frequency of mode l; g_i^l and g_{ij}^l the local and non-local electron-phonon couplings measuring the strength of interaction between holes (electrons) and intra-molecular and inter-molecular vibrations; and $\hat{a}_l^+(\hat{a}_l)$, the phonon creation (annihilation) operators, respectively. Eq. (1) implies harmonic modes and linear electron-phonon coupling[41] and the factor of $2^{-1/2}$ is included for consistency with other computational works referenced below. When realistic parameters for molecular semiconductors are considered, the local electron-phonon coupling causes the modulation of site energies while the non-local term leads to the fluctuation of the transfer integral which is typically of the same order of magnitude of the transfer integral itself, e.g., dynamic disorder.

The implementation of the transient localization theory requires the construction of a reference Hamiltonian including *static disorder* with statistical characteristics (variance and covariance of the expectation values of the electronic Hamiltonian) identical to that of dynamic disorder. We consider the quantum-mechanical thermal average of an arbitrary operator O over the lattice phonons,

$$\langle O\rangle = \frac{Tr[\exp(-H^{Ph}/k_B T)O]}{Tr[\exp(-H^{Ph}/k_B T)]} \quad (2)$$

where $H^{Ph} = \sum_l \hbar\omega_l(\hat{a}_l^{+}\hat{a}_l + \frac{1}{2})$ is the Hamiltonian of lattice phonons. Considering $\hat{J}_{ij} = J_{ij}^0 + \sum_l g_{ij}^l(a_l + a_l^{+})$, equation (2) can be implemented to evaluate the variance of transfer integral ($\sigma^2_{ij,T}$) as a global measure of its thermal fluctuations[42],

$$\sigma^2_{ij,T} = \left\langle (J_{ij} - \langle J_{ij}\rangle)^2 \right\rangle = \sum_l \frac{\left|g_{ij}^l\right|^2}{2} \coth\left(\frac{\hbar\omega_l}{2k_B T}\right) \quad (3)$$

where $k_B T$ indicates the thermal energy. It should be noted that the transient localization theory is a *high-temperature theory* in character as it does not account for phonon quantum effects and therefore breaks down at temperatures $k_B T \ll \hbar\omega_l$.

To analyse the correlation for pairs of intermolecular couplings that share a common molecule we use two quantities from bivariate statistics: the covariance and correlation coefficient. The covariance between the transfer integrals involving a common molecule is defined as,

$$cov(J_{ij}, J_{i'j'}) = \left\langle (J_{ij} - \langle J_{ij}\rangle).(J_{i'j'} - \langle J_{i'j'}\rangle) \right\rangle = \langle J_{ij}.J_{i'j'}\rangle - \langle J_{ij}\rangle\langle J_{i'j'}\rangle \quad (4)$$

when the expansion in normal phonon modes (eq. 3) is substituted in the covariance formula (eq. 4) one finds,

$$cov(J_{ij}, J_{i'j'}) = \sum_l \frac{g_{ij}^{l*} g_{i'j'}^l}{2} \coth\left(\frac{\hbar\omega_l}{2k_B T}\right) \quad (5)$$

The covariance itself does not depict immediate information and is usually divided against the standard deviations, leading to the Pearson correlation coefficient $\gamma_{ij,j'j'} = cov(J_{ij}, J_{i'j'}) \Big/ \sqrt{\sigma_{ij,T}\sigma_{i'j',T}}$.

Early applications of the theory assumed null covariance between pairs on the basis of computational observations indicating fairly small correlation coefficients[18]. We will assess the impact of this approximation in the results section.

The same *ab-initio* methods that yield fluctuations of J also provide fluctuations of the local energy at zero extra cost. Some of these modes are as slow as the intermolecular modes and

should be included in the evaluation of the mobility (in practice, by defining the relevant local energy fluctuations up to a suitable cut-off in the mode-frequency, one typically obtains diagonal fluctuations in the range ~10-50 meV at room temperature). However, this is not the focus of the present study and is, thus, not discussed in further detail. The interested reader is referred to Refs.[43–45].

When the transient localization theory is implemented for realistic systems one can evaluate explicitly the electron-phonon interaction matrix elements in the Hamiltonian eq. (1) (as done for example in[7,8,33,35,46–48]) and derive the variance and covariance from eq. (2)-(5) or directly compute the variance and covariance from computing the transfer integral along a molecular dynamics trajectory (as done for example in[18,34,49,50] and implemented in distributed software like VOTCA[51]).

Transient localization theory will be outlined for a generic 2D crystal (generalization to 3D is trivial) following the theory presented in Ref.[6]. According to the Kubo formula, a relation between the particle's mean-squared displacement (ΔX^2 (ΔY^2)) and the current correlations can be obtained through the retarded current-current anticommutator correlation function[52,53],

$$C_{+x(y)}(t) = \Theta(t)\left\langle \{\hat{j}_{x(y)}(t), \hat{j}_{x(y)}(0)\} \right\rangle \tag{6}$$

where $\Theta(t)$ is the Heaviside step function. Considering the current operator in terms of the velocity operator $\hat{j}_{x(y)} = -e\hat{V}_{x(y)} = -e\,dx(y)/dt$ and performing the time derivative, one can demonstrate that this function is directly related to the mean-squared displacement of the total position operator along the chosen direction:

$$\frac{d\Delta X^2(\Delta Y^2)(t)}{dt} = \frac{1}{e^2}\int_0^t C_{+x(y)}(t')dt' \tag{7}$$

with e being the elementary charge. The key step of the theory is the introduction of the Relaxation Time Approximation (RTA), i.e. the assumption that the dynamical properties of the electronic system can be expressed in terms of those of a reference system ($C_+^{ref}(t)$) from which it decays over time. The simplest possible form of RTA is $C_+(t) = C_+^{ref}(t)e^{-t/\tau}$, where the relaxation is determined by a single characteristic time capturing the timescale of the fluctuation of the electronic Hamiltonian. The reference system usually is defined as an idealized version of the

organic semiconductor with only static disorder, i.e., all the molecular displacements are frozen. The chosen form for the correlation function is correct in the short and the long time limit and can be seen as the simplest interpolation between the two. The success of the method can be ascribed to the weak dependence on the mobility on the parameter τ. This reference ensures that in the limit of large τ the system recovers the dynamics of a statically disordered system subject to Anderson localization.[54] On the other hand, upon introducing a finite relaxation time τ, the system recovers a diffusive behaviour at long time $t > \tau$, while it can show features of (transient) localization at shorter times. The relaxation time τ can be associated with the inverse of the typical intermolecular oscillation frequency ω_0 and it is customarily assumed that $\tau = \hbar/\omega_0$. Previous studies depict a distribution of intermolecular frequency modes typically peaked at $\hbar\omega_0 = \hbar/\tau = 5\,\text{meV}$ in several materials. In Ref.[27] the quantitative dependence of the mobility on the fluctuation time τ is investigated and it is shown that through variation of $\hbar/\tau$ between 2.5 and 10 meV, the L_τ^2/τ, which governs the mobility (eq. (10)), changes between 1.3 and 1. Therefore, one can conclude that the impact of τ on the mobility is rather weak which again justifies the validity of the chosen form of correlation function. Hence, the characteristic time of the transfer integral fluctuation has been set to a constant ($\hbar/\tau = \hbar\omega_0 = 5\,\text{meV}$). The chosen value corresponds to the typical value (within 15%) evaluated for all materials computed in Refs.[27,55].

We consider hole transport here and, therefore, in the Boltzmann statistics the significant contributions originate from the top edge of the band. The squared transient localization length attained at a time τ in *x* and *y* directions is given by,

$$L^2_{x(y)}(\tau) = \frac{1}{Z}\sum_{n,m} e^{\beta E_n} \left|\left\langle n \left| \hat{j}_{x(y)} \right| m \right\rangle\right|^2 \frac{2}{(\hbar/\tau)^2 + (E_m - E_n)^2} \tag{8}$$

with ($|n\rangle, |m\rangle$) and (E_n, E_m) being respectively the eigenstates and eigenvalues of the Hamiltonian in which dynamic disorder is replaced by static disorder of the same order of magnitude. $Z = \sum_n e^{\beta E_n}$ is the partition function with $\beta = 1/k_B T$. The current operator $\hat{j}$ along x and y directions, can be expressed in the energy eigenstatates' basis as follows,

$$\left\langle n\left|\hat{j}_{x(y)}\right|m\right\rangle = i\left\langle n\left|[\hat{H}, x(y)]\right|m\right\rangle = i(E_n - E_m)\left\langle n\left|x(y)\right|m\right\rangle \quad (9)$$

where x and y represent the position fluctuation in different directions. These steps give access to mobility through the Einstein relation in the framework of transient localization,

$$\mu_{x(y)} = \frac{e}{k_B T}\frac{\overline{L^2}_{x(y)}(\tau)}{2\tau} \quad (10)$$

with $\overline{L^2}_{x(y)}(\tau)$ being the disorder-averaged squared transient localization length[56]. In the following we shall report results for the average of the squared transient localization length over different directions,

$$\overline{L^2}(\tau) = \frac{\overline{L_x^2}(\tau) + \overline{L_y^2}(\tau)}{2}. \quad (11)$$

Practical Implementation

In practice, to implement the transient localization theory one may follow the following procedure:

1) Define a supercell of the system, i.e., the geometric position of all sites with appropriate periodic boundary conditions. The supercell size should be sufficiently large as discussed below.
2) Build a disordered electronic Hamiltonian of the size of the supercell with static disorder identical (in terms of variance and, eventually, correlations) to the dynamic disorder of the system.
3) Diagonalize the Hamiltonian and evaluate the transient localization length using eq. (8) and a fluctuation time τ.
4) Repeat steps 2)-3) *N* times with different realizations of disorder and compute *average* transient localization length. The statistical error on transient localization length can be made arbitrarily small by increasing the number of realizations.
5) Use eq. (10) to evaluate the mobility.

For the present method to be applicable, the size of the supercell should obviously be larger than the transient localization length. As the latter depends on the amount of disorder (which in turns depends on the temperature) one should check the convergence with the system size. We illustrate the procedure through a series of examples from simplified to more realistic models

requiring an increasing number of system-specific parameters.

3. Examples

Model Systems

To illustrate the procedure in a simple 2D case we consider the model proposed in Ref.[27] which provides the opportunity of studying a family of realistic model Hamiltonians. This is useful to visualize trends and avoid focusing on the peculiarity of one particular material. The model exploits the fact that almost all molecular semiconductors pack into crystal structures where one can determine a high-mobility plane, whereas the mobility perpendicular to the molecular layers in the same crystal is one to two orders of magnitude smaller [16]. Therefore, we shall consider a two-dimensional lattice with unit vectors ***a*** and ***b*** where each molecule is surrounded by six neighbours with only three distinct couplings (see Fig. 1.(I)).

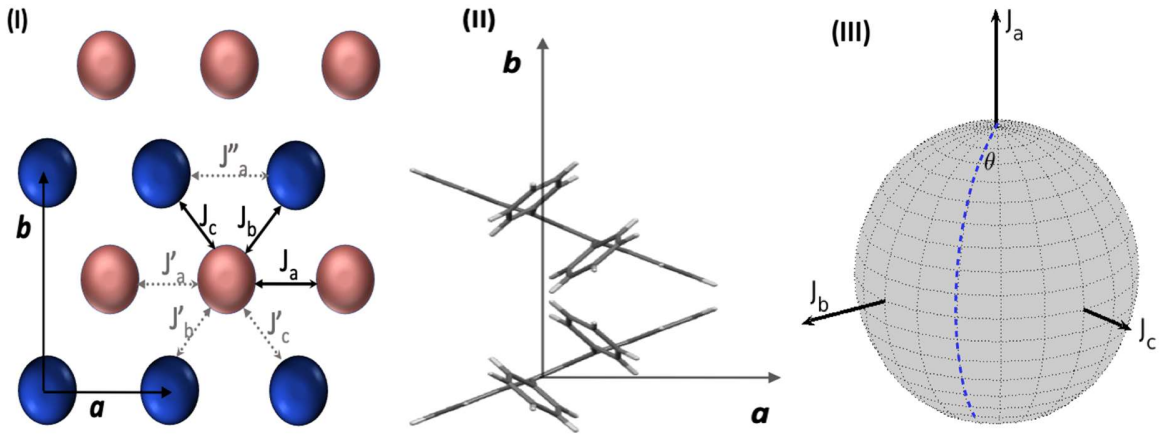

Figure 1: (I) A generic crystalline molecular structure with one molecule per site and three distinct nearest-neighbour electronic couplings J_a, J_b and J_c. The equivalent couplings are indicated by grey dashed lines and the same subscripts as the main ones. ***a*** and ***b*** denote the unit cell vectors. (II) Rubrene crystal structure with unit cell vectors ***a*** and ***b***. (III) Transfer integrals in different directions on the spherical surface defined by $J = J_a^2 + J_b^2 + J_c^2$ and the azimuthal angle $\theta = \cos^{-1}(J_a / J)$.

The average values of nearest-neighbour transfer integrals in three directions are indicated by J_a, J_b, J_c such that $J = J_a^2 + J_b^2 + J_c^2$ is a constant.

Hence, with a given set of transfer integrals, one can identify a one- to-one correspondence between points on a spherical surface and a molecular semiconductor.

The model as it is implemented in Ref.[27] provides an overall consistent picture of the transient localization properties of the molecular semiconductors. Here we benchmark the exact-diagonalization method represented in the preceding paragraphs by applying it to the model Hamiltonian of Ref.[27] recovering results obtained there via numerical simulations of the carrier quantum dynamics over time. In addition, we generalize the model in order to assess how the correlation between the transfer integrals affects the mobility. The present method is of much simpler applicability in practice, and, as we show below, it provides accurate results despite the limited sizes of the matrices that can be dealt via exact diagnolization.[57,58]

1) Uncorrelated transfer integrals

We study the tight-binding models described in Fig. (1) considering that the ratio between the fluctuation (standard deviation) and the average transfer integral is a constant for each coupling, i.e., $\Delta J_a / J_a = \Delta J_b / J_b = \Delta J_c / J_c \equiv \Delta J / J$ with ΔJ being the standard deviation of the distribution of the transfer integrals. We set $J = 0.1\,\text{eV}$ and assess a family of models with $J_a = J\cos(\theta)$ and $J_b = J_c = J\sin(\theta)/\sqrt{2}$ (see Fig. 1.(III)) as done in Ref.[27], defined by a single parameter $0 \le \theta \le \pi$. For example $\theta = 0, \pi$ describes a one-dimensional system with non-zero coupling only in one direction and $\theta = \theta_0 \cong 0.955$ represents an isotropic system (of higher symmetry) with equal transfer integral in the three directions. In addition, as was noted in Ref.[27], the value of the fluctuation time does not vary much between materials and its impact on the mobility is rather weak. Therefore, a characteristic time of molecular oscillation $\tau = 0.13\,\text{ps}$ ($\hbar/\tau = 5\,\text{meV}$) is considered throughout the calculation in this work. Also, the lattice parameters are set to ***a***=(1,0) and ***b***=(0, $\sqrt{3}$) (results for different unit cell sizes can be forwardly obtained by simple rescaling). The key quantity of interest is the squared localization length averaged over several realizations of disorder. Figure (2) reproduces the results shown in Ref.[27]

depicting the variation of the localization length versus the azimuthal angle θ.

Here a supercell of size 25*25 is considered and the temperature, disorder strength and number of realization of disorder are set to $T = 290\,K$, $\sigma = \Delta J / J = 0.5$ and $N = 50$, respectively. It has to be noted that the unit cell is composed of two molecules which is a common occurrence in molecular semiconductors; therefore the mentioned supercell contains 1250 molecules. In Ref.[27] instead, a supercell of size 200*200 was used. The number of atoms does not play specific role in this methodology. As depicted in the inset, the squared localization lengths are normally distributed and one can compute them with any target accuracy by increasing N. With $N = 50$, the largest standard deviation of $L^2(\tau)$ is 2.3% of its average value. Recovering what was obtained in Ref.[27], the smallest localization is observed for the one-dimensional structures as expected[59,60]. On the other hand, the localization effects are weakest at the point θ_0 which corresponds to more isotropic band structures (nearest neighbours transfer integrals are as close as possible in absolute value and their product has a positive sign)[59] leading to a robust behaviour against dynamic disorder and therefore larger transient localization lengths and mobilities.

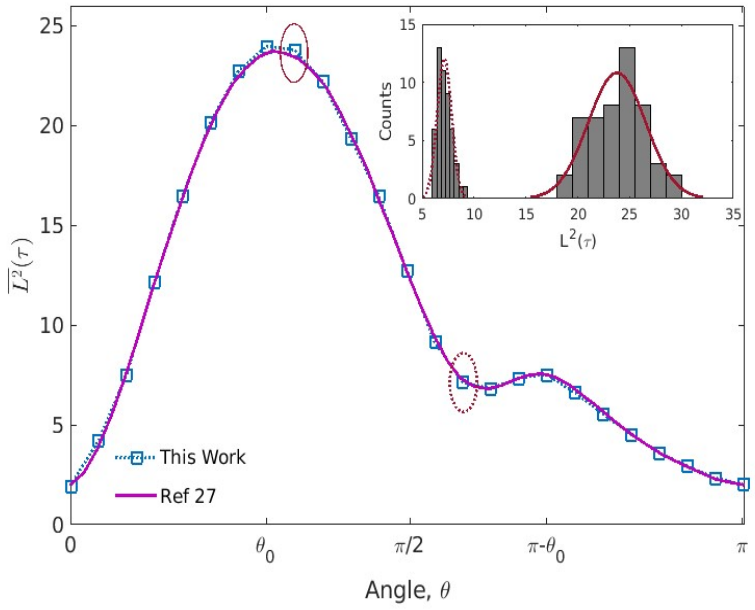

Figure 2: Squared transient localization length calculated based on eq. (8) in the absence of couplings correlation. Inset represents the distribution of data marked with circles in the main panel.

The localization lengths are in terms of unit cells unless another unit is mentioned explicitly. It has to be noted that the system Hamiltonian (eq. (1)) contains certain symmetry elements due to the arbitrary phase of the molecular orbitals (MO). If the sign of a MO is changed two transfer integrals change sign, and the systems with the so-changed transfer integrals is undistinguishable from the original. On the other hand, changing sign of just one transfer integral of the three is not a symmetry operation and therefore such a system will have different eigenvalues, DOS, effective mass, etc. This explains the asymmetric behavior of the curve in Fig. (2) with respect to $\pi/2$ as this is equivalent to changing the sign of just one transfer integral (not achievable by changing the sign of any MO). The described behavior is a property of the band structure and it is unrelated to the theory proposed here.

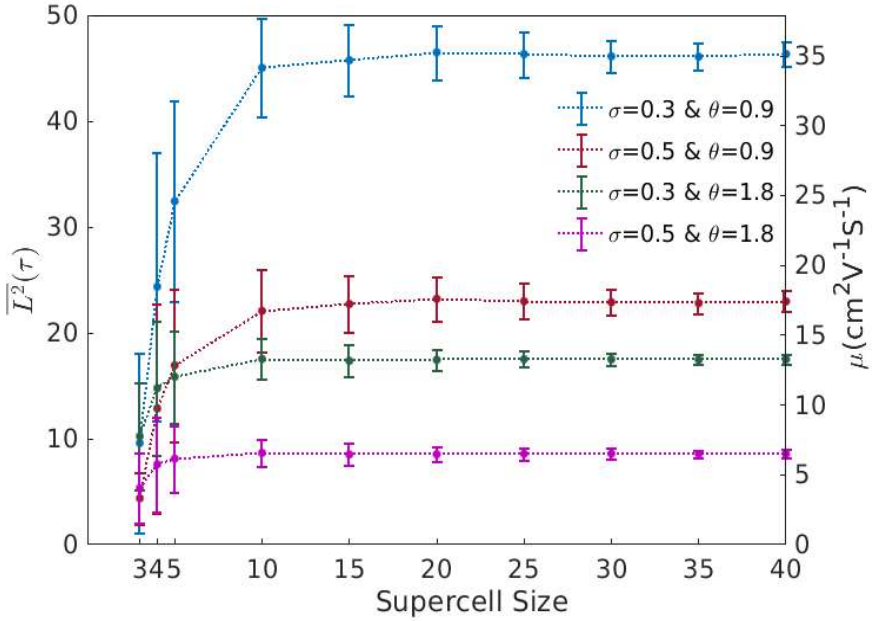

Figure 3: Squared transient localization length calculated for different supercell size (different number of molecules) at two disorder strengths namely $\sigma = 0.3$ and $\sigma = 0.5$ around $\theta = 0.9$ and $\theta = 1.8$. The x-axis denotes the supercell linear size (supercell is a square) and shown are error bars defined as "standard deviation over N realizations of disorder" which is conceivable as a consequence of normal distribution of $L^2(\tau)$ as represented in Fig. (2). The mobility unit is set by $(e/k_B T)a^2/2\tau = 0.76\ cm^2V^{-1}S^{-1}$ with $a = 7A^0$ being the lattice spacing.

As previously mentioned, to guarantee the applicability of the method, the size of the supercell should obviously be larger than the squared transient localization length. This is substantiated in

Fig. (3), illustrating the convergence with the system size. As can be seen, in typical situations of interest the rate of convergence is rapid (achieved even with a supercell of size 20*20) and high accuracy is attainable with a growing size of supercell and smaller localization lengths. This implies that for low disorder the method is limited by the ability of diagonalizing large matrices and the user of the code must check it for convergence. As a critical point, in a computer system with a memory of 15 GB, the code breaks down for systems of size greater than 69*69. For the rest of the paper we present results with system size 25*25 and 50 realizations of disorder to achieve a good balance between accuracy and computational speed.

II) Correlated transfer integrals

This section focuses on evaluating transient localization in the presence of arbitrary correlation between transfer integrals involving a common molecule. We use the Cholesky decomposition algorithm as a general approach to produce random data with arbitrary correlation. To generate k number of correlated normally distributed random variables, with N observations, given a positive (semi-) definite correlation matrix R_{k*k}, one needs to finding a matrix M_{k*k} such that $M^{+}M=R$, where M is computed by the Cholesky decomposition for symmetric positive definite R[61–63]. Then, after generating a matrix of uncorrelated and normally distributed variables U_{N*k}, the matrix $(UM)_{N*k}$ contains a N observation of k normally distributed variables with the desired correlation.

To explore systematically the effect of correlation we consider the same model of the previous section and assume that the correlation between any two matrix elements is γ, if they share a common index (i.e., a common molecule), and zero otherwise. Therefore, this parameter allows us to study the system in the presence of an arbitrary amount of correlation. It should be noted that the paradigmatic 1D case with one mode per molecule, which has been studied in depth[4,5,64,65] corresponds to $\gamma=0.5$[60]. It has to be noted that with multiple modes with positive and negative correlation one can have all correlations between -0.5 and 0.5.

Figure (4) compares the squared localization length of correlated systems with the case of null correlation. The following points are notable: (i) the localization length decreases in the presence of transfer integrals correlation (the stronger the correlation the smaller the mobility).

Intuitively this can be rationalized considering that strong positive correlation in a system with all positive transfer integrals is equivalent to a strong amplification of the disorder, with sites more strongly or more weakly coupled with all their neighbours at the same time, (ii) the decrease in localization length is larger in the region of the high symmetry point θ_0.

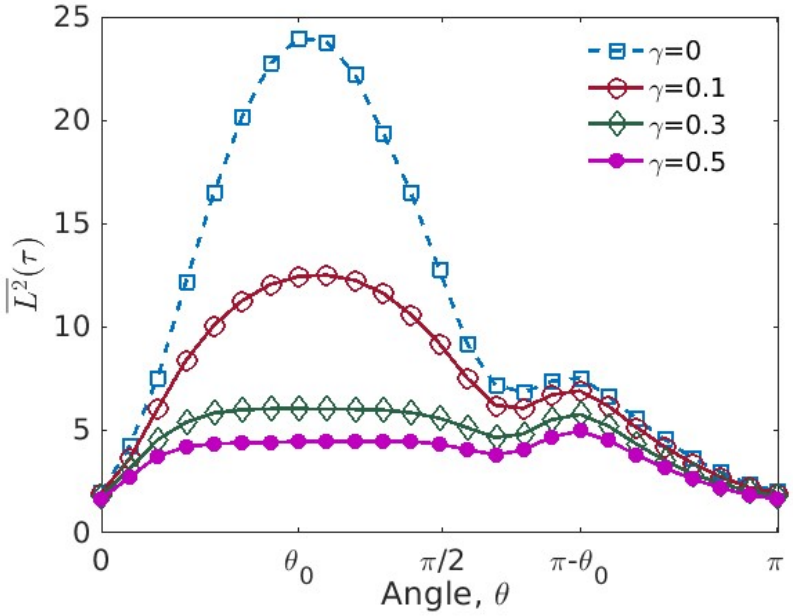

Figure 4: Squared transient localization calculated upon varying the amount of correlation between the thermal fluctuations of transfer integrals.

Realistic Systems: Correlation derived from non-local electron-phonon coupling

To compute the localization length in realistic systems (whether correlated or uncorrelated) the first step involves the Hamiltonian construction based on the real electronic couplings. We have used the electronic couplings presented in Ref[66] where the transfer integrals of Tetracene and Rubrene molecular semiconductors are computed by employing the localized highest-occupied molecular orbital (HOMO) of each moiety at the studied molecular pair. Calculations of the transfer integrals are carried out performing *ab-initio* calculations at the B3LYP/6-31G* level of theory as implemented in Gaussian 09[67]. To assess the impact of correlation in realistic systems, based on eq. (2)-(5) one has to use the nonlocal electron-phonon couplings (g_{ij}^{l}) and phonon frequencies (ω_l) to extract the correlation coefficient between different molecular pairs ($\gamma_{ij,i'j'}$). We use the nonlocal electron-phonon coupling for the prototypical molecular semiconductor

Rubrene and Tetracene (two of the best performing molecular semiconductors[68]). The values of g_{ij}^{I} and ω_I are extracted from Ref.[66] in which the phonon modes are obtained from quantum chemical methods[69,70] and a supercell approach[71,72] is implemented for sampling the momentum space to avoid mixing the intra- and intermolecular modes. We wish to include the correlation between transfer integrals that involve at least one common molecule. Fig. 1(II) illustrates the minimum number of transfer integrals in addition to J_a, J_b, J_c that need to be considered. They are shown in grey and indicated as $J_a'(J_a'')$, J_b', J_c' as their respective equivalent couplings. Furthermore, as $J_b = J_c$ therefore, $J_b' = J_c'$. The standard deviation σ of $J_a(J_b)$ in Rubrene was found to increase from 44.88 (8.54) meV to 58.71 (11.00) meV with rising temperature from $T = 200\,K$ to $T = 350\,K$ which is consistent with the $\sigma \propto \sqrt{T}$ rule (cf. eq. 3) and with previously published data [66,73]. Within the same temperature window, the standard deviation σ of J_a, J_b, J_c in Tetracence was increased from 23.0, 12.8, 23.8 meV to 29.6, 16.3, 30.2 meV which is in accordance with the data presented in Ref [74]. In Table I and II, the correlation coefficients in Rubrene and Teracene, between the couplings sharing a molecule are listed. As can be seen, the symmetry of the system is reflected in the correlation coefficients, i.e., the equivalent couplings such as ($J_a J_b$) and ($J_a' J_b'$) exhibit the same correlation coefficient. It has to be noted that, although the symmetry is preserved in the correlation coefficients leading to some identical coefficients but one cannot consider a constant single correlation value for a realistic material, which was the main assumption in the above presented model system. The correlation coefficients are generally very small, both positive and negative, with the largest coefficient being just below 0.2 found for the $J_a J_b'$ pair in Rubrene and 0.268 for $J_a J_c$ in Teracene.

It has to be noted that the sign of the correlation coefficient is not arbitrary and it is uniquely set by the choice of sign of the MO basis. Once the sign of the transfer integral are computed consistently, they can be presented in four alternative ways, e.g. the original sign and the sign of J_a, J_b or J_a, J_c or J_b, J_c changed but not in any possible way. The sign of the correlation coefficient depends on the choice of the sign of the transfer integral but they cannot be changed arbitrarily, if the sign of one MO is changed, the sign of all transfer integral involving

that MO will change and the correlation between a given J_1 and J_2 will change sign if only one transfer integral between J_1 or J_2 has changed sign.

Table 1: The correlation coefficient for pairs of intermolecular couplings in rubrene that involve a common molecule at $T = 290\,K$.

	J_a	J_b	J_c	J'_a	J'_b	J'_c	J''_a
J_a	1	0.166	0.013	0.197	0.022	-0.025	0
J_b	0.166	1	-0.007	0.022	-0.036	-0.039	0.117
J_c	0.013	-0.007	1	0.021	-0.039	0.008	0.095
J'_a	0.197	0.022	0.021	1	0.166	0.013	0
J'_b	0.022	-0.036	-0.039	0.166	1	-0.007	0
J'_c	-0.025	-0.039	0.008	0.013	-0.007	1	0
J''_a	0	0.117	0.095	0	0	0	1

Table 2: The correlation coefficient for pairs of intermolecular couplings in tetracene that involve a common molecule at $T = 290\,K$.

	J_a	J_b	J_c	J'_a	J'_b	J'_c	J''_a
J_a	1	0.188	0.268	-0.046	-0.028	-0.106	0
J_b	0.188	1	-0.121	-0.028	-0.008	0.016	0.003
J_c	0.268	-0.121	1	-0.107	0.016	-0.235	0.015
J'_a	-0.046	-0.028	-0.107	1	0.188	0.268	0
J'_b	-0.028	-0.008	0.016	0.188	1	-0.121	0
J'_c	-0.106	0.016	-0.235	0.268	-0.121	1	0
J''_a	0	0.003	0.015	0	0	0	1

Figure (5) depicts squared localization length and its components for a range of temperatures in the absence and presence of correlation for two realistic systems named Rubrene and Tetracene. In both cases, in the absence of correlation, the values of diagonal elements $L_x^2(\tau)$ and $L_y^2(\tau)$ and consequently $L^2(\tau)$ diminish upon increasing temperature as a result of the increase in thermal disorder. The weak correlation between couplings reported in Table I and Table II leads to a slight reduction of the transient localization length, as well as to a smoother variation versus temperature. Overall, however, the differences between correlated and uncorrelated case are modest and possibly below the foreseeable ability to discriminate between models when comparing with experiment. To compute the mobility for a set of squared localization length and temperature one has to substitute these values in eq.(10). For instance, through substituting the temperature 290K and squared localization length 408 $\mathring{A}^2$ and 295.5 $\mathring{A}^2$ for Rubrene and Tetracene one can obtain the mobility 6.3 cm^2/Vs and 4.5 cm^2/Vs, respectively.

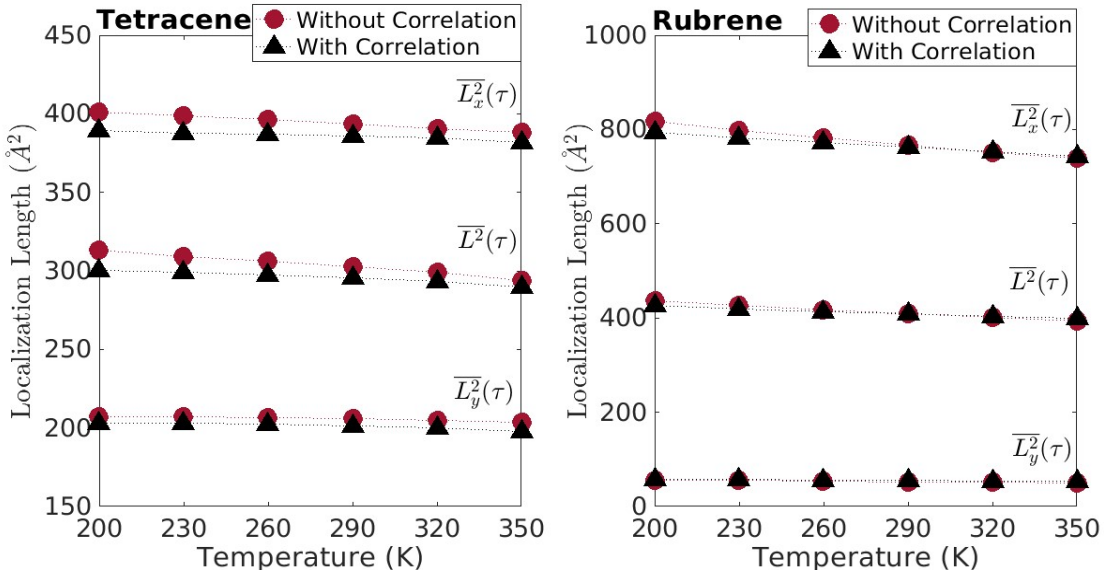

Figure 5: Temperature dependence of the squared localization length and its components in the absence and presence of couplings correlation. The unit of localization length is squared Angstroms.

The localization reported with experimental studies such as electron spin resonance (ESR)[75] methods is very compatible with the transient localization. The spatial extent of the spin density

distribution (wavefunction) of the carriers evaluated from the ESR line-width reveals to be in the order of 10-20 molecules[76,77]. However it is important to keep separated the quantitative concept of transient localization which is derived from Kubo-Greenwood equation and is therefore probed by measures of mobility and other "localization lengths" which can be dependent on the method used to probe the carrier (its characteristic time, the presence of selection rule, the role of defect states). The connection with other experimental evaluations of localization length is to be considered only qualitative before the appropriate spectroscopic theory is developed. The most extensive comparison with experimental mobility (considering 8 materials) and discussion of the sources of error is presented in detail in Ref.[27]. Relying on the analysis performed in Ref.[27] and considering few recent measurements, reported in Ref.[78,79], one can see that for Rubrene in spite of different fabrication techniques the charge carrier mobility data are similar and reasonable averaged experimental mobility can be estimated by 8.6 cm^2/Vs. In contrast, very few studies on Tetracene have been performed and the maximum of 2.4 cm^2/Vs has been reached by today which is smaller than the predicted theoretical values[80]. This point was indicated previously in other theoretical works[81].

4.Conclusions

In conclusion, we provide a step-by-step efficient procedure to calculate the charge mobility of molecular semiconductors in the framework of transient localization theory. The method is practically simple to implement and produces results that are fully equivalent to the standard formulation of the theory in terms of the quantum dynamics of charge carriers. The computational cost is that of a repeated direct diagonalization of matrices of moderate size with excellent convergence properties. The connection with routine results from electronic structure calculations is immediate and was exemplified here for the case of Rubrene and Tetracene. As an illustration of the method flexibility, we have examined the presence of correlation in the thermal fluctuation of transfer. This effect is found to cause a reduction of the mobility although the effect is very small when the specific examples are considered. This new implementation is sufficiently fast to allow for rapid screening of new materials and can be considered alongside alternative quantum propagation methods.

Supporting Information available. A sample code to reproduce the results in Figure 2 and two data sets containing the nonlocal electron-phonon coupling for Rubrene and Tetracene are available. A version of the code that will be maintained/updated is available at the Github repository https://github.com/CiuK1469/TransLoc.

Acknowledgments. This work was supported by the ERC through Grant No. 615834. T.N. would like to thank Dr. Didier Mayou for fruitful discussions.

References:

(1) Troisi, A. Charge Transport in High Mobility Molecular Semiconductors: Classical Models and New Theories. *Chem. Soc. Rev.* **2011**, *40* (5), 2347.
(2) Brédas, J. L.; Norton, J. E.; Cornil, J.; Coropceanu, V. Molecular Understanding of Organic Solar Cells: The Challenges. *Acc. Chem. Res.* **2009**, *42* (11), 1691–1699.
(3) Oberhofer, H.; Reuter, K.; Blumberger, J. Charge Transport in Molecular Materials: An Assessment of Computational Methods. *Chem. Rev.* **2017**, *117* (15), 10319–10357.
(4) Coropceanu, V.; Cornil, J.; da Silva Filho, D. A.; Olivier, Y.; Silbey, R.; Brédas, J. L. Charge Transport in Organic Semiconductors. *Chem. Rev.* **2007**, *107* (4), 926–952.
(5) Troisi, A.; Orlandi, G. Charge-Transport Regime of Crystalline Organic Semiconductors: Diffusion Limited by Thermal off-Diagonal Electronic Disorder. *Phys. Rev. Lett.* **2006**, *96* (8), 1–4.
(6) Fratini, S.; Mayou, D.; Ciuchi, S. The Transient Localization Scenario for Charge Transport in Crystalline Organic Materials. *Adv. Funct. Mater.* **2016**, *26* (14), 2292–2315.
(7) Yi, Y.; Coropceanu, V.; Brédas, J. L. Nonlocal Electron-Phonon Coupling in the Pentacene Crystal: Beyond the Γ-Point Approximation. *J. Chem. Phys.* **2012**, *137* (16).
(8) Martinelli, N. G.; Olivier, Y.; Athanasopoulos, S.; Delgado, M. R.; Pigg, K. R.; Da Silva Filho, D. A.; Sánchezcarrera, R. S.; Venuti, E.; Delia Valle, R. G.; Brédas, J. L.; et al. Influence of Intermolecular Vibrations on the Electronic Coupling in Organic Semiconductors: The Case of Anthracene and Perfluoropentacene. *ChemPhysChem* **2009**, *10* (13), 2265–2273.
(9) Ortmann, F.; Bechstedt, F.; Hannewald, K. Charge Transport in Organic Crystals: Interplay of Band Transport, Hopping and Electron-Phonon Scattering. *New J. Phys.* **2010**, *12*, 0–7.
(10) Blülle, B.; Troisi, A.; Häusermann, R.; Batlogg, B. Charge Transport Perpendicular to the High Mobility Plane in Organic Crystals: Bandlike Temperature Dependence Maintained despite Hundredfold Anisotropy. *Phys. Rev. B* **2016**, *93* (3), 035205.
(11) Bussolotti, F.; Yang, J.; Yamaguchi, T.; Yonezawa, K.; Sato, K.; Matsunami, M.; Tanaka, K.; Nakayama, Y.; Ishii, H.; Ueno, N.; et al. Hole-Phonon Coupling Effect on the Band Dispersion of Organic Molecular Semiconductors. *Nat. Commun.* **2017**, *8* (1).
(12) Illig, S.; Eggeman, A. S.; Troisi, A.; Jiang, L.; Warwick, C.; Nikolka, M.; Schweicher, G.; Yeates, S. G.; Henri Geerts, Y.; Anthony, J. E.; et al. Reducing Dynamic Disorder in Small-Molecule Organic Semiconductors by Suppressing Large-Amplitude Thermal Motions. *Nat. Commun.* **2016**, *7*, 1–10.
(13) Shuai, Z.; Wang, L.; Li, Q. Evaluation of Charge Mobility in Organic Materials: From Localized to Delocalized Descriptions at a First-Principles Level. *Adv. Mater.* **2011**, *23* (9), 1145–1153.
(14) Yang, X.; Li, Q.; Shuai, Z. Theoretical Modelling of Carrier Transports in Molecular Semiconductors: Molecular Design of Triphenylamine Dimer Systems. *Nanotechnology* **2007**, *18* (42).

(15) Yang, H.; Gajdos, F.; Blumberger, J. Intermolecular Charge Transfer Parameters, Electron-Phonon Couplings, and the Validity of Polaron Hopping Models in Organic Semiconducting Crystals: Rubrene, Pentacene, and C60. *J. Phys. Chem. C* **2017**, *121* (14), 7689–7696.
(16) Difley, S.; Wang, L.; Yeganeh, S.; Yost, S. R.; Voorhis, T. V. A. N. Electronic Properties of Disordered Organic Semiconductors via QM / MM Simulations. **2010**, *43* (7), 995–1004.
(17) Shuai, Z.; Geng, H.; Xu, W.; Liao, Y.; André, J. M. From Charge Transport Parameters to Charge Mobility in Organic Semiconductors through Multiscale Simulation. *Chem. Soc. Rev.* **2014**, *43* (8), 2662–2679.
(18) Troisi, A.; Orlandi, G. Dynamics of the Intermolecular Transfer Integral in Crystalline Organic Semiconductors. *J. Phys. Chem. A* **2006**, *110* (11), 4065–4070.
(19) Gajdos, F.; Oberhofer, H.; Dupuis, M.; Blumberger, J. On the Inapplicability of Electron-Hopping Models for the Organic Semiconductor Phenyl-C61-Butyric Acid Methyl Ester (PCBM). *J. Phys. Chem. Lett.* **2013**, *4* (6), 1012–1017.
(20) Koh, S. E.; Risko, C.; Da Silva Filho, D. A.; Kwon, O.; Facchetti, A.; Brédas, J. L.; Marks, T. J.; Ratner, M. A. Modeling Electron and Hole Transport in Fluoroarene-Oligothiopene Semiconductors: Investigation of Geometric and Electronic Structure Properties. *Adv. Funct. Mater.* **2008**, *18* (2), 332–340.
(21) Giannini, S.; Carof, A.; Blumberger, J. Crossover from Hopping to Band-Like Charge Transport in an Organic Semiconductor Model: Atomistic Nonadiabatic Molecular Dynamics Simulation. *J. Phys. Chem. Lett.* **2018**, *9* (11), 3116–3123.
(22) Bai, X.; Qiu, J.; Wang, L. An Efficient Solution to the Decoherence Enhanced Trivial Crossing Problem in Surface Hopping. *J. Chem. Phys.* **2018**, *148* (10).
(23) Spencer, J.; Gajdos, F.; Blumberger, J. FOB-SH: Fragment Orbital-Based Surface Hopping for Charge Carrier Transport in Organic and Biological Molecules and Materials. *J. Chem. Phys.* **2016**, *145* (6).
(24) Heck, A.; Kranz, J. J.; Kubař, T.; Elstner, M. Multi-Scale Approach to Non-Adiabatic Charge Transport in High-Mobility Organic Semiconductors. *J. Chem. Theory Comput.* **2015**, *11* (11), 5068–5082.
(25) Ren, J.; Vukmirović, N.; Wang, L. W. Nonadiabatic Molecular Dynamics Simulation for Carrier Transport in a Pentathiophene Butyric Acid Monolayer. *Phys. Rev. B* **2013**, *87* (20), 1–14.
(26) Wang, L.; Beljonne, D. Flexible Surface Hopping Approach to Model the Crossover from Hopping to Band-like Transport in Organic Crystals. *J. Phys. Chem. Lett.* **2013**, *4* (11), 1888–1894.
(27) Fratini, S.; Ciuchi, S.; Mayou, D.; de Laissardière, G. T.; Troisi, A. A Map of High-Mobility Molecular Semiconductors. *Nat. Mater.* **2017**, *16* (10), 998–1002.
(28) Mayou, D.; Khanna, S.; Mayou, D.; Approach, S. K. A. R.; Journal, T. A Real-Space Approach to Electronic Transport To Cite This Version : HAL Id : Jpa-00247129. **1995**, *5* (9), 1199–1211.
(29) Hart, G. L. W.; Blum, V.; Walorski, M. J.; Zunger, A. Evolutionary Approach for Determining First-Principles Hamiltonians. *Nat. Mater.* **2005**, *4* (5), 391–394.
(30) Ordejón, P.; Boskovic, D.; Panhans, M.; Ortmann, F. Ab Initio Study of Electron-Phonon Coupling in Rubrene. *Phys. Rev. B* **2017**, *96* (3), 1–9.
(31) Li, Y.; Coropceanu, V.; Brédas, J. L. Nonlocal Electron-Phonon Coupling in Organic Semiconductor Crystals: The Role of Acoustic Lattice Vibrations. *J. Chem. Phys.* **2013**, *138* (20).
(32) Munn, R. W.; Silbey, R. Theory of Electronic Transport in Molecular Crystals. II. Zeroth Order States Incorporating Nonlocal Linear Electron-Phonon Coupling. *J. Chem. Phys.* **1985**, *83* (4), 1843–1853.
(33) Girlando, A.; Grisanti, L.; Masino, M.; Bilotti, I.; Brillante, A.; Della Valle, R. G.; Venuti, E. Peierls and Holstein Carrier-Phonon Coupling in Crystalline Rubrene. *Phys. Rev. B* **2010**, *82* (3), 1–8.
(34) Wang, L.; Prezhdo, O. V.; Beljonne, D. Mixed Quantum-Classical Dynamics for Charge Transport in

Organics. *Phys. Chem. Chem. Phys.* **2015**, *17* (19), 12395–12406.
(35) Shuai, Z.; Geng, H.; Xu, W.; Liao, Y.; André, J.-M. From Charge Transport Parameters to Charge Mobility in Organic Semiconductors through Multiscale Simulation. *Chem. Soc. Rev.* **2014**, *43* (8), 2662.
(36) Hannewald, K.; Stojanović, V. M.; Schellekens, J. M. T.; Bobbert, P. A.; Kresse, G.; Hafner, J. Theory of Polaron Bandwidth Narrowing in Organic Molecular Crystals. *Phys. Rev. B* **2004**, *69* (7), 1–7.
(37) Atta-Fynn, R.; Biswas, P.; Drabold, D. A. Electron-Phonon Coupling Is Large for Localized States. *Phys. Rev. B* **2004**, *69* (24), 1–5.
(38) Markussen, T.; Palsgaard, M.; Stradi, D.; Gunst, T.; Brandbyge, M.; Stokbro, K. Electron-Phonon Scattering from Green's Function Transport Combined with Molecular Dynamics: Applications to Mobility Predictions. *Phys. Rev. B* **2017**, *95* (24), 1–8.
(39) Novikov, S. V; Dunlap, D. H.; Kenkre, V. M.; Parris, P. E.; Vannikov, A. V. Essential Role of Correlations in Governing Charge Transport in Disordered Organic Materials. **1998**, *1* (4), 3–6.
(40) Li, Y.; Yi, Y.; Coropceanu, V.; Br, J. Symmetry Effects on Nonlocal Electron-Phonon Coupling in Organic Semiconductors. **2012**, *245201*, 1–7.
(41) Eggeman, A. S.; Illig, S.; Troisi, A.; Sirringhaus, H.; Midgley, P. A. Measurement of Molecular Motion in Organic Semiconductors by Thermal Diffuse Electron Scattering. *Nat. Mater.* **2013**, *12* (11), 1045–1049.
(42) Coropceanu, V.; Sánchez-Carrera, R. S.; Paramonov, P.; Day, G. M.; Brédas, J.-L. Interaction of Charge Carriers with Lattice Vibrations in Organic Molecular Semiconductors: Naphthalene as a Case Study. *J. Phys. Chem. C* **2009**, *113* (11), 4679–4686.
(43) Fratini, S.; Ciuchi, S. Dynamical Mean-Field Theory of Transport of Small Polarons. *Phys. Rev. Lett.* **2003**, *91* (25), 256403.
(44) Silbey, R.; Munn, R. W. General Theory of Electronic Transport in Molecular Crystals. I. Local Linear Electron-Phonon Coupling. *J. Chem. Phys.* **1980**, *72* (4), 2763–2773.
(45) Lee, N. E.; Zhou, J. J.; Agapito, L. A.; Bernardi, M. Charge Transport in Organic Molecular Semiconductors from First Principles: The Bandlike Hole Mobility in a Naphthalene Crystal. *Phys. Rev. B* **2018**, *97* (11), 1–8.
(46) Coropceanu, V.; Li, Y.; Yi, Y.; Zhu, L.; Brédas, J. L. Intrinsic Charge Transport in Single Crystals of Organic Molecular Semiconductors: A Theoretical Perspective. *MRS Bull.* **2013**, *38* (1), 57–64.
(47) Wang, L.; Li, Q.; Shuai, Z.; Chen, L.; Shi, Q. Multiscale Study of Charge Mobility of Organic Semiconductor with Dynamic Disorders. *Phys. Chem. Chem. Phys.* **2010**, *12* (13), 3309.
(48) Schweicher, G.; Olivier, Y.; Lemaur, V.; Geerts, Y. H. What Currently Limits Charge Carrier Mobility in Crystals of Molecular Semiconductors? *Isr. J. Chem.* **2014**, *54* (5–6), 595–620.
(49) Zhu, L.; Geng, H.; Yi, Y.; Wei, Z. Charge Transport in Organic Donor–Acceptor Mixed-Stack Crystals: The Role of Nonlocal Electron–Phonon Couplings. *Phys. Chem. Chem. Phys.* **2017**, *19* (6), 4418–4425.
(50) Akimov, A. V. Libra: An Open-Source "Methodology Discovery" Library for Quantum and Classical Dynamics Simulations. *J. Comput. Chem.* **2016**, *37* (17), 1626–1649.
(51) Ru, V.; Junghans, C.; Lukyanov, A.; Kremer, K.; Andrienko, D. Versatile Object-Oriented Toolkit for Coarse-Graining Applications. **2009**, 3211–3223.
(52) Fratini, S.; Ciuchi, S.; Mayou, D. Phenomenological Model for Charge Dynamics and Optical Response of Disordered Systems: Application to Organic Semiconductors. **2014**, 1–11.
(53) Ciuchi, S.; Fratini, S.; Mayou, D. Transient Localization in Crystalline Organic Semiconductors. *Phys. Rev. B* **2011**, *83* (8), 1–4.
(54) Anderson, P. W. Local Moments and Localized States. *Rev. Mod. Phys.* **1978**, *50* (2), 191–201.
(55) Harrelson, T. F.; Dantanarayana, V.; Xie, X.; Koshnick, C.; Nai, D.; Fair, R.; Nuñez, S. A.; Thomas, A. K.; Murrey, T. L.; Hickner, M. A.; et al. Direct Probe of the Nuclear Modes Limiting Charge Mobility

in Molecular Semiconductors. *Mater. Horizons* **2018**, 182–191.
(56) **Note:** The average over disorder can be performed in the "annealed" sense if we consider classical vibration by performing a separate sum on all displacement configurations in both numerator and denominator (Z) of Eq. (8). Alternatively, considering frozen disorder requires a "quenched" average, i.e., averaging the numerator and denominator of Eq. (8) simultaneously. However, for sufficiently large cells the difference between the two methods is negligible.
(57) Roche, S.; Mayou, D. A New Formalism for the Computation of RKKY Interaction in Aperiodic Systems. **1999**.
(58) Triozon, F.; Vidal, J.; Mosseri, R.; Mayou, D. Quantum Dynamics in Two- and Three-Dimensional Quasiperiodic Tilings. *Phys. Rev. B* **2002**, *65* (22), 2202021–2202024.
(59) Lee, P. A.; Ramakrishnan, T. V. Disordered Electronic Systems. *Rev. Mod. Phys.* **1985**, *57* (2), 287–337.
(60) Troisi, A. Dynamic Disorder in Molecular Semiconductors: Charge Transport in Two Dimensions. *J. Chem. Phys.* **2011**, *134* (3).
(61) Pourahmadi, M.; Daniels, M. J.; Park, T. Simultaneous Modelling of the Cholesky Decomposition of Several Covariance Matrices. *J. Multivar. Anal.* **2007**, *98* (3), 568–587.
(62) Loehlin, J. C. The Cholesky Approach: A Cautionary Note. *Behav. Genet.* **1996**, *26* (1), 65–69.
(63) Elman, H. C.; Ramage, A.; Silvester, D. J. Algorithm 866. *ACM Trans. Math. Softw.* **2007**, *33* (2), 14–es.
(64) Fratini, S.; Ciuchi, S. Bandlike Motion and Mobility Saturation in Organic Molecular Semiconductors. *Phys. Rev. Lett.* **2009**, *103* (26), 1–4.
(65) Ciuchi, S.; Fratini, S. Electronic Transport and Quantum Localization Effects in Organic Semiconductors. *Phys. Rev. B* **2012**, *86* (24), 1–14.
(66) Xie, X.; Santana-Bonilla, A.; Troisi, A. Nonlocal Electron-Phonon Coupling in Prototypical Molecular Semiconductors from First Principles. *J. Chem. Theory Comput.* **2018**, acs.jctc.8b00235.
(67) Frisch, M. J.; Trucks, G. W.; Schlegel, H. B.; Scuseria, G. E.; Robb, M. A.; Cheeseman, J. R.; Scalmani, G.; Barone, V.; Mennucci, B.; Petersson, G. A.; et al. Gaussian 09, Revision A. 1. *Gaussian Inc. Wallingford CT* **2009**, *27*, 34.
(68) Facchetti, A. Semiconductors for Organic Transistors. *Mater. Today* **2007**, *10* (3), 28–37.
(69) Jurchescu, O. D.; Meetsma, A.; Palstra, T. T. M. Low-Temperature Structure of Rubrene Single Crystals Grown by Vapor Transport. *Electrochem. Solid-State Lett.* **2006**, *9* (5), 330–334.
(70) Holmes, D.; Kumaraswamy, S.; Matzger, A. J.; Vollhardt, K. P. C. On the Nature of Nonplanarity in the [N] Phenylenes. *Chem. Eur. J.* **1999**, *5*, 3399–3412.
(71) Yi, Y.; Coropceanu, V.; Brédas, J. L. Nonlocal Electron-Phonon Coupling in the Pentacene Crystal: Beyond the Γ-Point Approximation. *J. Chem. Phys.* **2012**, *137* (16).
(72) Medrano Sandonas, L.; Teich, D.; Gutierrez, R.; Lorenz, T.; Pecchia, A.; Seifert, G.; Cuniberti, G. Anisotropic Thermoelectric Response in Two-Dimensional Puckered Structures. *J. Phys. Chem. C* **2016**, *120* (33), 18841–18849.
(73) Troisi, A. Prediction of the Absolute Charge Mobility of Molecular Semiconductors: The Case of Rubrene. *Adv. Mater.* **2007**, *19* (15), 2000–2004.
(74) Landi, A.; Troisi, A. Rapid Evaluation of Dynamic Electronic Disorder in Molecular Semiconductors. *J. Phys. Chem. C* **2018**, *122*, 18336–18345.
(75) Wertz, J. *Electron Spin Resonance: Elementary Theory and Practical Applications*; Springer Science & Business Media, 2012.
(76) Marumoto, K.; Kuroda, S. I.; Takenobu, T.; Iwasa, Y. Spatial Extent of Wave Functions of Gate-Induced Hole Carriers in Pentacene Field-Effect Devices as Investigated by Electron Spin Resonance. *Phys. Rev. Lett.* **2006**, *97* (25), 2–5.
(77) Matsui, H.; Mishchenko, A. S.; Hasegawa, T. Distribution of Localized States from Fine Analysis of

Electron Spin Resonance Spectra in Organic Transistors. *Phys. Rev. Lett.* **2010**, *104* (5), 1–4.
(78) Xie, W.; McGarry, K. A.; Liu, F.; Wu, Y.; Ruden, P. P.; Douglas, C. J.; Frisbie, C. D. High-Mobility Transistors Based on Single Crystals of Isotopically Substituted Rubrene- d 28. *J. Phys. Chem. C* **2013**, *117* (22), 11522–11529.
(79) Blülle, B.; Häusermann, R.; Batlogg, B. Approaching the Trap-Free Limit in Organic Single-Crystal Field-Effect Transistors. *Phys. Rev. Appl.* **2014**, *1* (3), 1–8.
(80) Reese, C.; Chung, W. J.; Ling, M. M.; Roberts, M.; Bao, Z. High-Performance Microscale Single-Crystal Transistors by Lithography on an Elastomer Dielectric. *Appl. Phys. Lett.* **2006**, *89* (20).
(81) Deng, W. Q.; Goddard, W. A. Predictions of Hole Mobilities in Oligoacene Organic Semiconductors from Quantum Mechanical Calculations. *J. Phys. Chem. B* **2004**, *108* (25), 8614–8621.

TOC Graphic: